Supplemental Dataset:

Mechanism of the Intrinsic Arginine Finger in Heterotrimeric G-Proteins

Daniel Mann, Christian Teuber, Stefan Tennigkeit, Grit Schröter, Klaus Gerwert, and Carsten Kötting

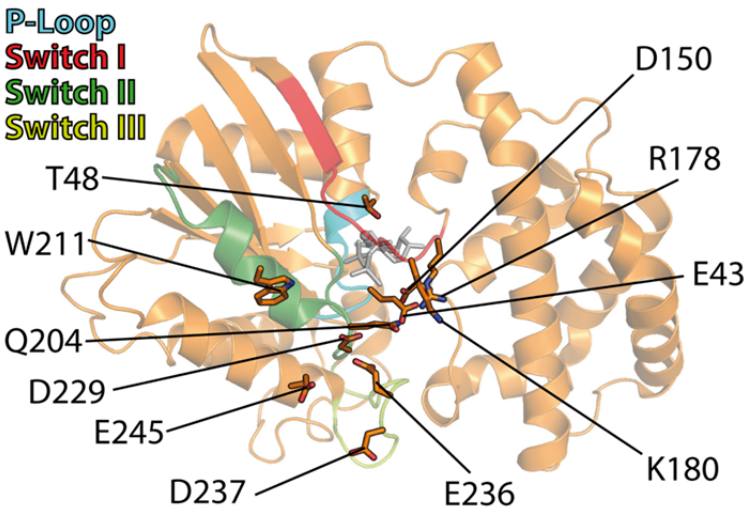

Supplemental Figure 1: Locations of the investigated point mutants in $G\alpha_{i1}$ (PDB-ID 1GIA)

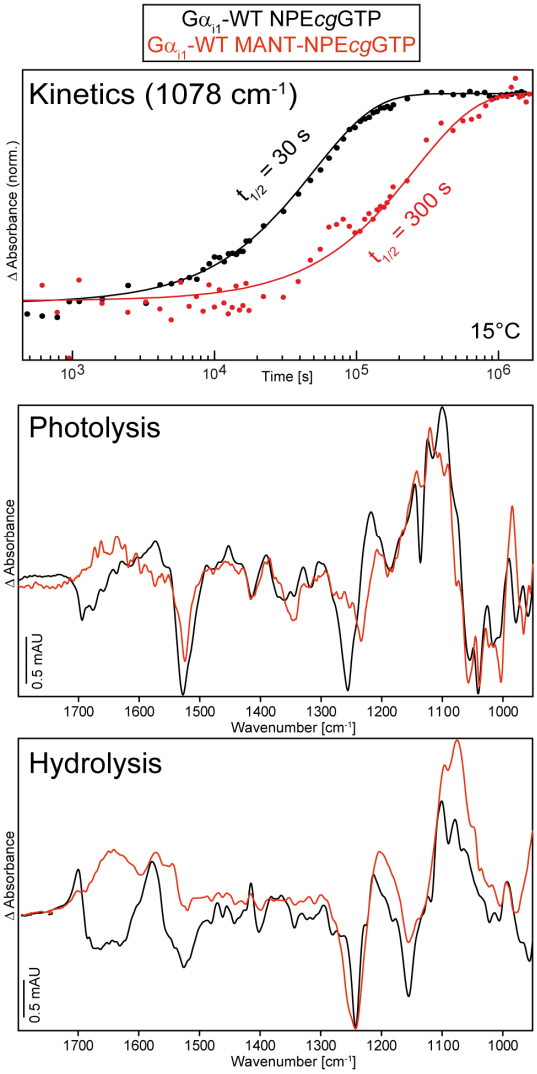

Supplemental Figure 2: Exchange of GTP to MANT-GTP significantly alters kinetics and infrared spectra of $G\alpha_{i1}$-WT

Positive bands in the photolysis correspond to the GTP state, negative bands correspond to the caged-GTP state. Positive bands in the hydrolysis reaction represent the GDP state of $G\alpha_{i1}$ whereas negative bands represent the GTP state.

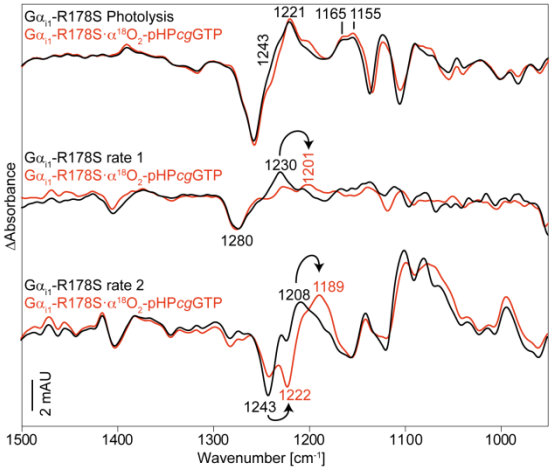

Supplemental Figure 3: Assignment of IR bands of α-GTP and α-GDP in $G\alpha_{i1}$-R178S in H_2O

Positive bands in the photolysis correspond to the GTP state, negative bands correspond to the caged-GTP state. Positive bands in rate 1 and 2 of the hydrolysis reaction represent the GDP state of $G\alpha_{i1}$-R178S whereas negative bands represent the GTP state. Arrows indicate band shifts caused by the heavy isotopes.

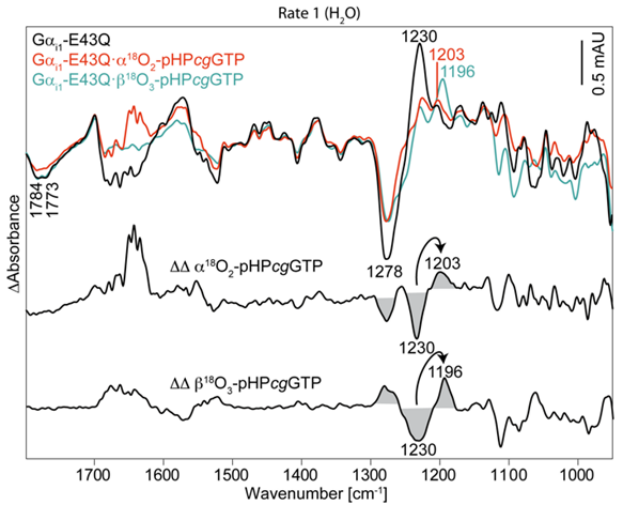

Supplemental Figure 4: $\alpha^{18}O_2$ pHP*cg*GTP and $\beta^{18}O_3$ pHP*cg*GTP labeling of the rate that preceded hydrolysis in $G\alpha_{i1}$-E43Q

The mutant $G\alpha_{i1}$-E43Q shows an additional rate that precedes the hydrolysis reaction. Isotopic labeling using $\alpha^{18}O_2$ pHP*cg*GTP and $\beta^{18}O_3$ pHP*cg*GTP showed that the band at 1230 cm^{-1} is caused by α- and β-GTP. Double differences ($\Delta\Delta$) are the result of labeled minus unlabeled spectra. Arrows indicate band shifts caused by the heavy ^{18}O isotopes.

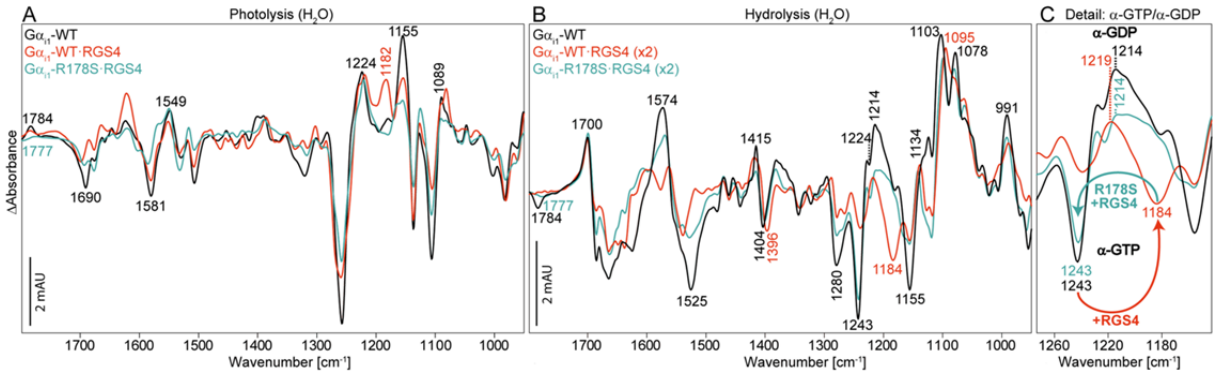

Supplemental Figure 5: Photolysis (A) and Hydrolysis (B) spectra of intrinsic and RGS4 catalyzed $G\alpha_{i1}$-WT and the mutant $G\alpha_{i1}$-R178S. RGS4 addition shifts the α-GTP vibration to lower wavenumbers. This effect is reversible when Arg178 is mutated (C).

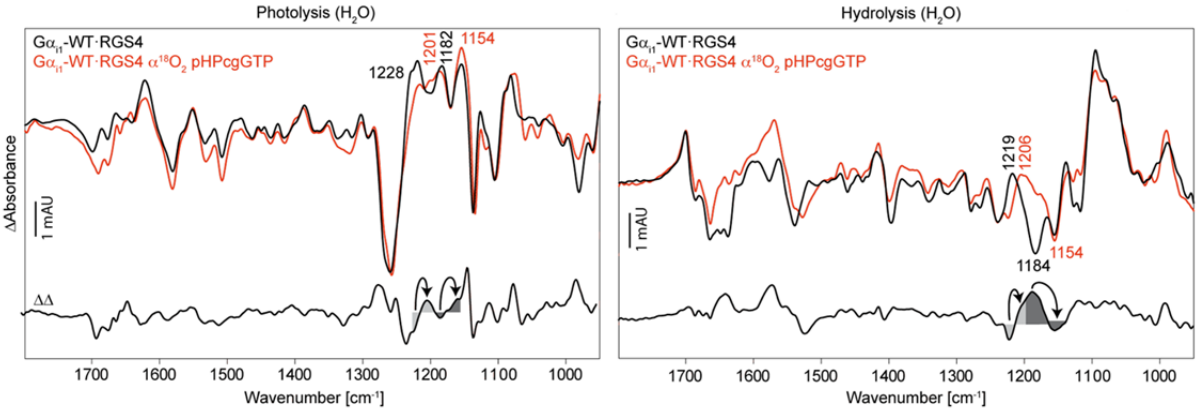

Supplemental Figure 6: α-GTP / α-GDP band assignments of $G\alpha_{i1}$·RGS4 in H_2O

Positive bands in the photolysis correspond to the GTP state, negative bands correspond to the caged-GTP state. Positive bands in the hydrolysis reaction represent the GDP state of $G\alpha_{i1}$·RGS4 whereas negative bands represent the GTP state. Arrows indicate band shifts caused by the heavy isotopes.

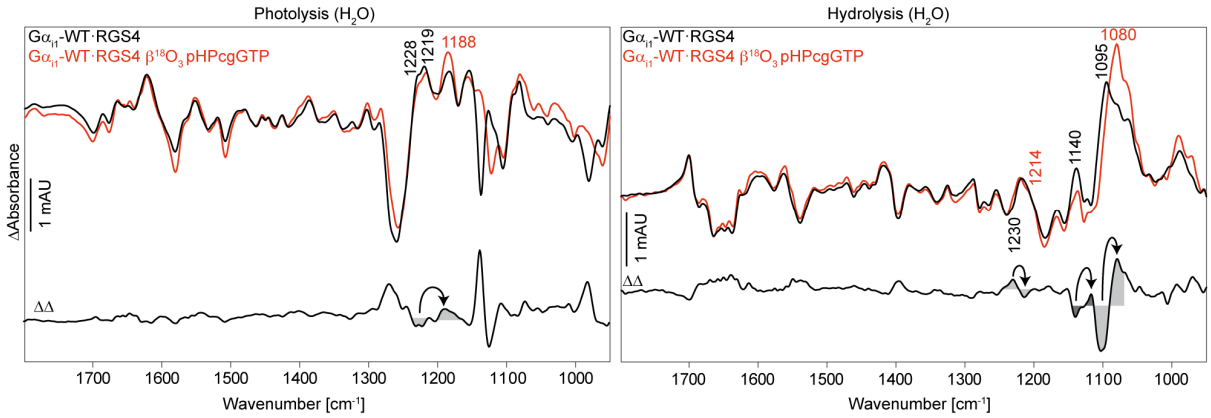

Supplemental Figure 7: β-GTP / β-GDP band assignments of $G\alpha_{i1}$·RGS4 in H_2O

Positive bands in the photolysis correspond to the GTP state, negative bands correspond to the caged-GTP state. Positive bands in the hydrolysis reaction represent the GDP state of $G\alpha_{i1}$·RGS4 whereas negative bands represent the GTP state. Arrows indicate band shifts caused by the heavy isotopes.

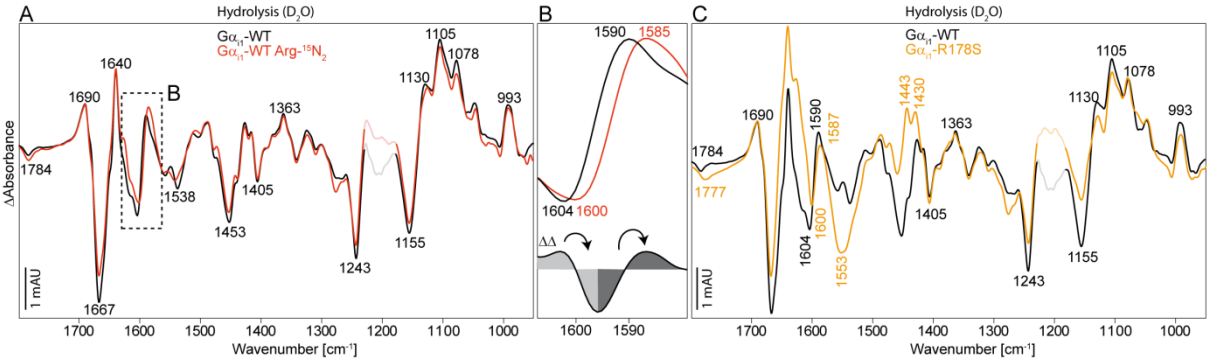

Supplemental Figure 8: Infrared band assignment of $G\alpha_{i1}$-Arg178

Deuterated hydrolysis spectra of unlabeled (black) and $\eta^{15}N_2$-Arg labeled $G\alpha_{i1}$ (A). Detailed view (B) and double difference spectrum ($\Delta\Delta$) of the assignment. The bands at 1604 cm^{-1} (GTP state) and 1590 cm^{-1} (GDP state) are assigned to Arg178. This assignment is site specific since the bands were also missing in the mutant $G\alpha_{i1}$-R178S (C). Positive bands correspond to the GDP state, negative bands correspond to the GTP state. Arrows indicate band shifts caused by the heavy isotopes. Grayed out areas are superimposed by DOD bending of deuterated water.

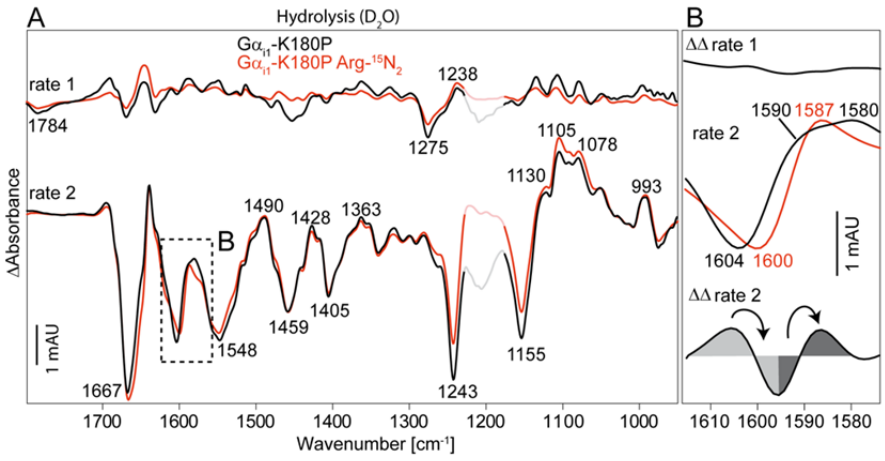

Supplemental Figure 9: Infrared band assignment of $G\alpha_{i1}$-Arg178 in the rate separated mutant $G\alpha_{i1}$-K180P

A: rate 1 and 2 of unlabeled (black) and $\eta^{15}N_2$-Arg labeled $G\alpha_{i1}$-K180P (red). B: double differences ($\Delta\Delta$) of rate 1 show a zero-line, exclusively rate 2 shows isotopic shifts for the bands 1604 cm^{-1} and 1590 cm^{-1} like in wildtype $G\alpha_{i1}$. Positive bands correspond to the GDP state, negative bands correspond to the GTP state

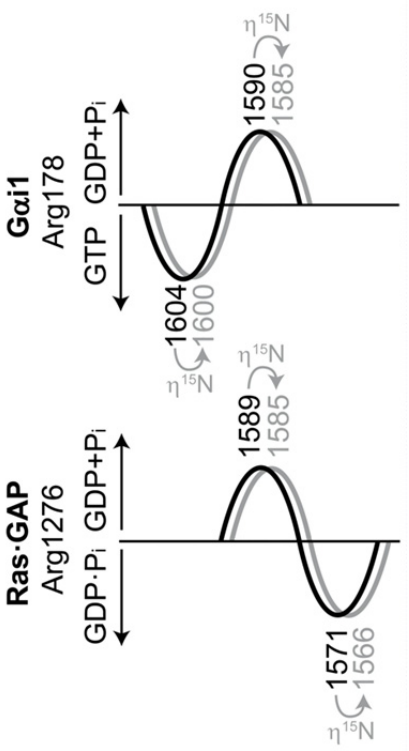

Supplemental Figure 10: Infrared bands of the arginine finger in $G\alpha_{i1}$ and Ras·GAP and their corresponding $\eta^{15}N_2$ shifts (gray) in comparison.

In $G\alpha_{i1}$ 1604 cm^{-1} represents the GTP-bound state of the arginine finger whereas 1590 cm^{-1} represents the GDP state. In Ras•GAP 1589 cm^{-1} represents the arginine in a water environment whereas 1571 cm^{-1} represents the arginine finger within the binding pocket but after bond beakage (17). The GTP bound state is not resolved in Ras•GAP and could now be resolved for the first time in $G\alpha_{i1}$.

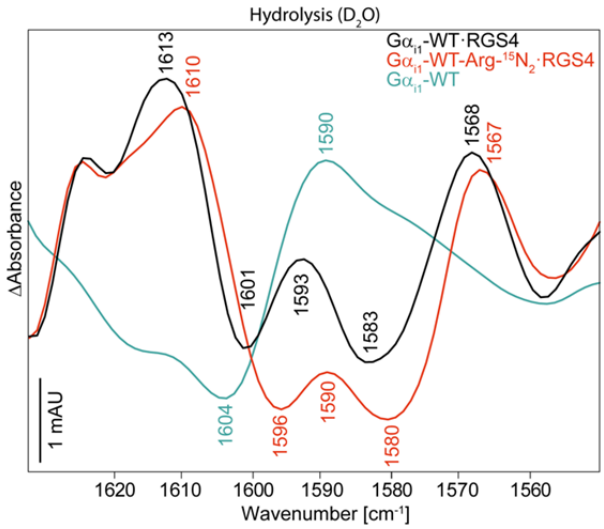

Supplemental Figure 11: Isotopic labeling of the arginine finger in RGS4 catalyzed FTIR measurements of $G\alpha_{i1}$.

The intrinsic vibrations of Arg178 at 1604 and 1590 cm^{-1} were no longer observable when RGS4 was added, probably due to altered GTP coordination. Positive bands represent the GDP state whereas negative bands represent the GTP state.

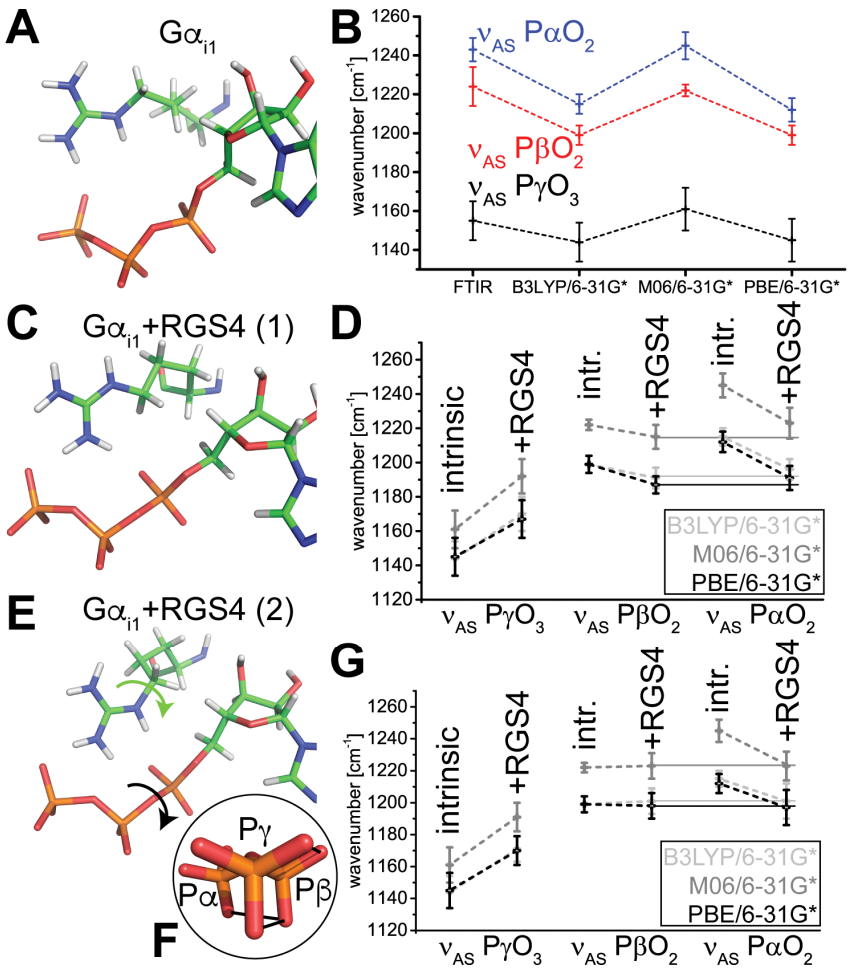

Supplemental Figure 12: QM/MM calculations of $G\alpha_{i1}$ and $G\alpha_{i1}$-RGS4.

Intrinsic (A) and RGS4 catalyzed $G\alpha_{i1}$ (C,E) and the corresponding calculated IR spectra from QM/MM simulations (B,D,G). QM/MM spectra calculation (B) of intrinsic $G\alpha_{i1}$-GTP (A) on the levels B3LYP/6-31G*, M06/6-31G* and PBE/6-31G* in comparison to the experiment (FTIR). Shown are mean values and standard deviations for 15 snapshots of a 100 ns MD simulation. (D,G) Shown are RGS4 induced α-, β- and γ-GTP shifts for configurations (C) and (E), respectively. Calculation of configuration (E) resulted in eclipsed (α-β-γ)-GTP (F). While calculation of geometry (C) with RGS4 resulted in higher α-GTP vibrations in comparison to the β-GTP vibrations (solid lines) this trend is reversed (G) for the eclipsed geometry (E) (solid lines) which is in line with the experiment. All spectra were scaled according to CCCBDB (B3LYP/6-31G*: 0.96; M06/6-31G*: 0.95; PBE/6-31G*: 0.99).

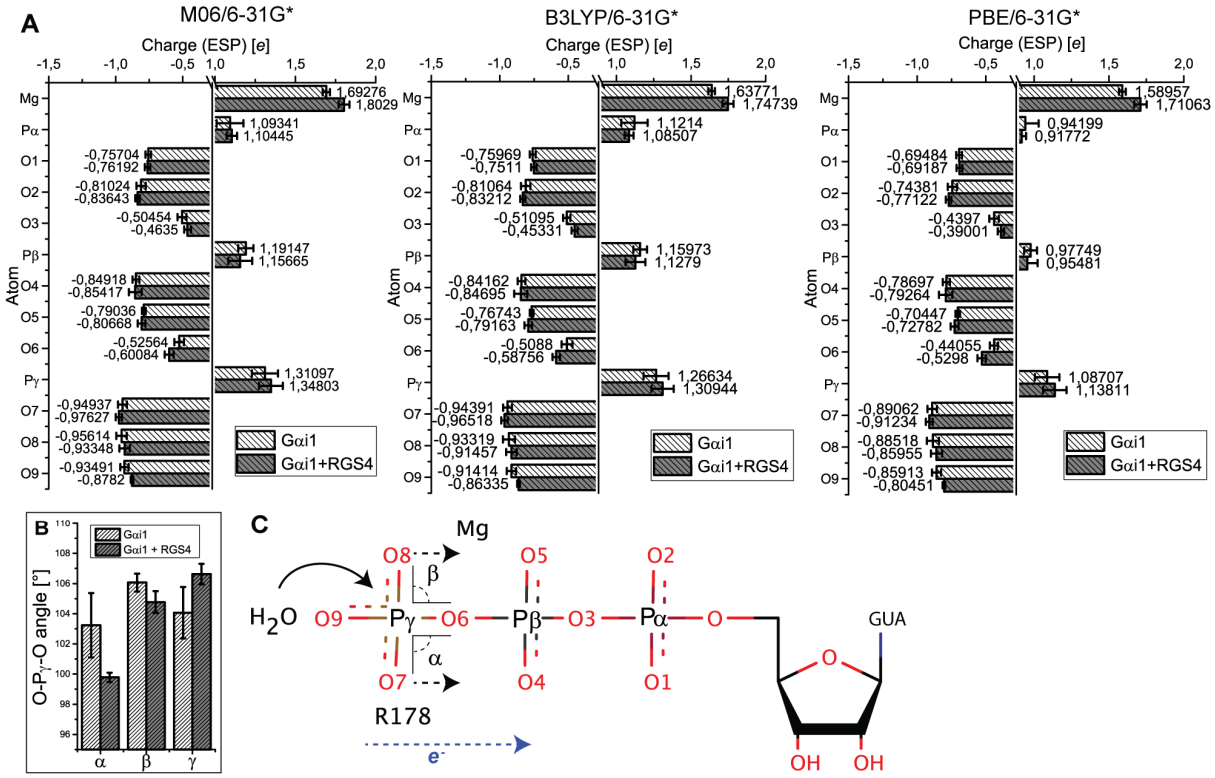

Supplemental Figure 13: Detailed ESP Charge distribution of intrinsic and RGS4 bound $G\alpha_{i1}$

(A) ESP partial charges of intrinsic and RGS4 bound $G\alpha_{i1}$ on the levels B3LYP/6-31G*, M06/6-31G* and PBE/6-31G*. Charge is transferred towards the bridging β-γ-GTP oxygen (O6). Atom names match those in panel (C). (B) planarity of γ-GTP is increased when RGS4 is bound.

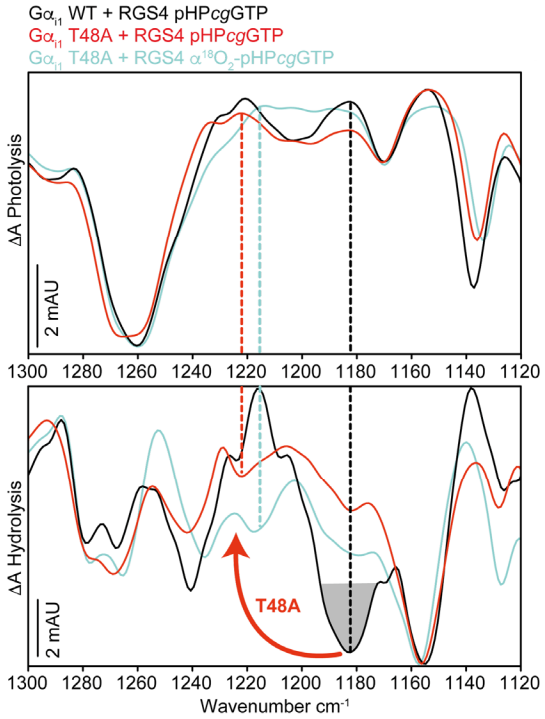

Supplemental Figure 14: Band assignment of α-GTP for the mutant $G\alpha_{i1}$-T48A+RGS4.

In $G\alpha_{i1}$-T48A+RGS4 the α-GTP band is shifted from 1184 cm^{-1} to 1220 cm^{-1}, indicating the RGS4 induced 59 cm^{-1} α-GTP band shift is caused by strong binding of α-GTP between Arg178 and Thr48.

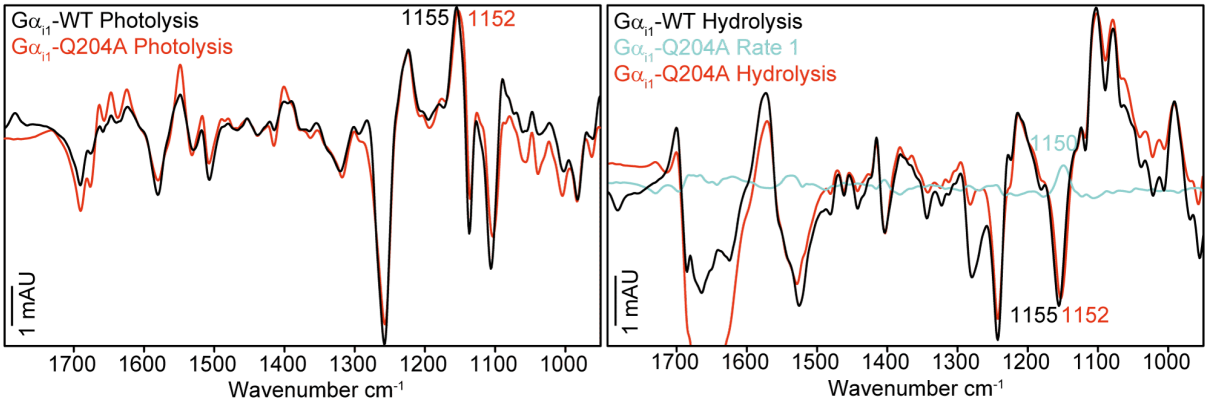

Supplemental Figure 15: FTIR measurements of $G\alpha_{i1}$-WT and $G\alpha_{i1}$-Q204A

Photolysis and hydrolysis spectra almost match completely. The γ-GTP band at 1155 cm^{-1} is slightly red-shifted to 1152 cm^{-1} and $G\alpha_{i1}$-Q204A shows an intermediate rate with a spectral feature at 1150 cm^{-1}. Half-live values of global fits are depicted in Table 1.

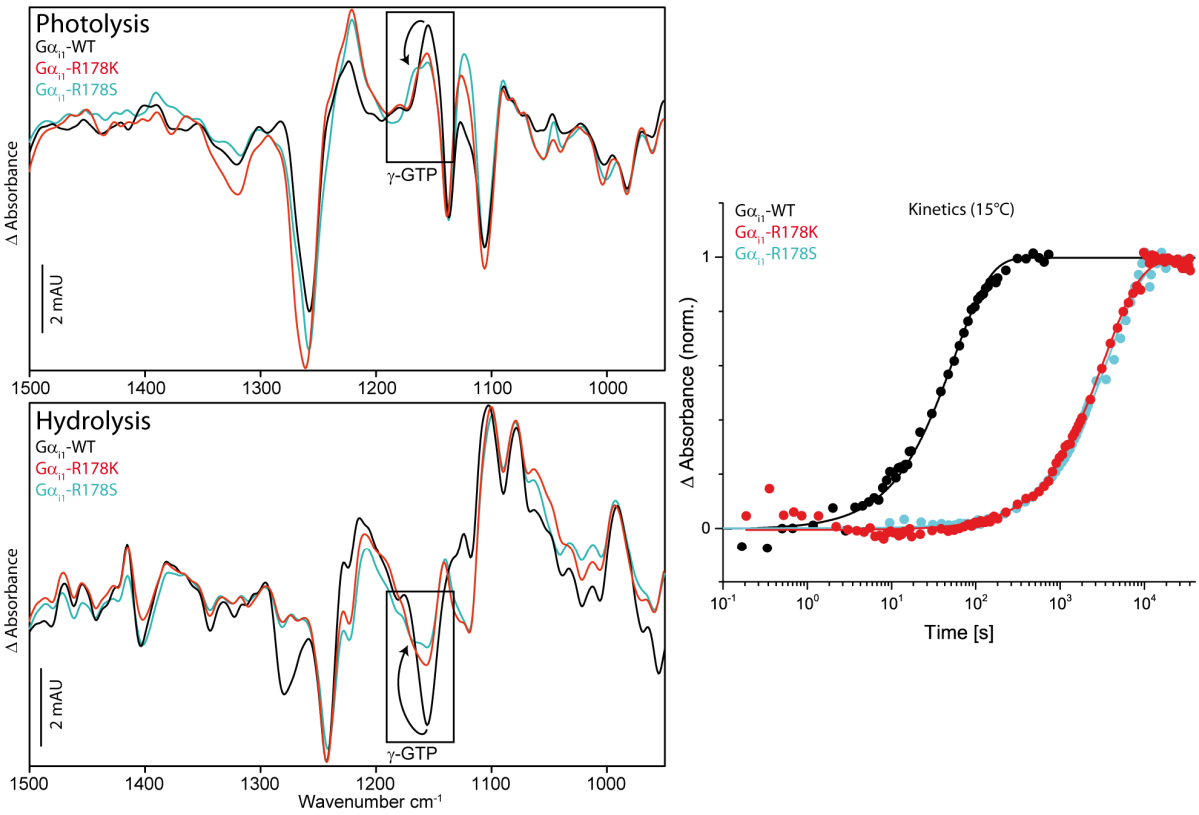

Supplemental Figure 16: FTIR measurements of $G\alpha_{i1}$-R178K

The γ-GTP vibration of $G\alpha_{i1}$-R178K resembles more the $G\alpha_{i1}$-WT γ-GTP vibration at 1155 cm^{-1} than the γ-GTP vibration of $G\alpha_{i1}$-R178S, probably indicating that Lys178 is also bound to γ-GTP. However, hydrolysis kinetics are comparably slowed down, indicating not only the charge of the arginine finger is important but also its geometry.

	Σ Pγ-O_3	(Pγ-) O(-Pβ)	Σ Pβ-O_2	(Pβ-) O (-Pα)	Σ Pα-O_2
$G\alpha_{i1}$	-1.53	-0.52	-0.45	-0.50	-0.48
$G\alpha_{i1}$+RGS4	-1.45	-0.60	-0.50	-0.46	-0.50

Supplemental Table 1: Charge sums (ESP) in QM/MM calculations (M06/6-31G*)